X is given by

$$K_X=\frac{M_0}{2\mu_B}(H_{\rm hf})_X\chi(A_1+A_2+\cdots)\xi_X a_X^2, \quad \text{(A2)}$$

where A_1, A_2, $\cdots$ are the atomic weights of the atoms at the respective sites, and ξ_X is the ratio of the hyperfine field at site X in the metal to its value in the free atom. The sum $\sum_X \xi_X a_X^2$ should be a number of order unity.

For V_3X, the unit cell contains six V atoms and two X atoms. From Eq. (A2) we have

$$K_{\rm V}=\frac{M_0}{2\mu_B}(H_{\rm hf})_{\rm V}\chi(A_{\rm V}+\tfrac{1}{3}A_X)(6a_{\rm V}^2\xi_{\rm V}), \quad \text{(A3)}$$

$$K_X=\frac{M_0}{2\mu_B}(H_{\rm hf})_X\chi(3A_{\rm V}+A_X)(2a_X^2\xi_X), \quad \text{(A4)}$$

with $(6a_{\rm V}^2\xi_{\rm V})+(2a_X^2\xi_X)\simeq 1$. With some changes in notation this is the result used in the text.

PHYSICAL REVIEW VOLUME 121, NUMBER 5 MARCH 1, 1961

Fine Structure of Secondary Emission vs Angle of Incidence of the Primary Beam on Titanium Single Crystals*

R. W. Sosheat† and A. J. Dekker‡
Department of Electrical Engineering, University of Minnesota, Minneapolis, Minnesota
(Received May 16, 1960; revised manuscript received November 21, 1960)

The secondary emission ratio of single crystals of titanium has been measured as a function of the angle of incidence of the primary electron beam. The curves show a general increase of the secondary emission ratio with increasing angle between the electron beam and the normal to the crystal face. Superimposed upon this general increase are a number of small relative maxima. The larger and broader of these maxima occur whenever the primary beam is incident along one of the major zone axes of the crystal. The magnitudes of these bands vary with the energy of the incident electrons, but their angular position is independent of energy. The smaller, extremely narrow bands do not correspond to major zone axes of the crystal. Both the magnitude and angular position of these latter peaks vary with the primary energy. The origin of these bands is explained in terms of diffraction of the incident electrons by the crystal lattice.

INTRODUCTION

THE curves of the secondary emission ratio, δ, of titanium crystals vs the angle, θ, between the primary beam and the normal to the crystal surface show fine structure superimposed on a smooth variation. This fine structure appears when the primary beam is directed approximately along a principal zone axis, and its angular position is independent of the energy of the primary electrons. This type of effect was first discovered on MgO crystals by Laponsky and Whetten.[1] The data on titanium also show smaller, narrower peaks, called ultrafine structure, whose angular position varies with primary energy. The structure in the curves was studied for angles of incidence up to $\pm 60°$ and for primary energies from 120 ev to 10 kev. It appears that both the "normal" fine structure and the ultrafine structure can be explained in terms of diffraction of the primary electrons in the surface layers of the crystal.[2]

I. EXPERIMENTAL PROCEDURE

The magnitudes of the peaks in the curves of δ vs θ range from the order of 1% to 20% of the total secondary yield. Thus, in order to obtain precise quantitative data on the magnitude, width, and position of these peaks it is necessary to measure the total yield with considerable accuracy. The basic electron circuit which is employed in these measurements is shown in Fig. 1. The primary beam, I_p, leaving the electron gun passes through a small hole in the collector and strikes the target, producing secondary electrons. The secondaries are emitted at all angles and have energies ranging from zero to that of the primary electrons. When the collector is at a positive potential with respect to the target, all of the secondaries are collected and the ratio of I_c to I_p is the total secondary emission ratio which we represent by "δ". When the bridge circuit in Fig. 1 is balanced, the ratio of I_c to I_p is proportional to the value of the setting on the ten-turn potentiometer (for values of δ not exceeding 2), and thus can be determined quite accurately.

* Based on a thesis submitted in partial fulfillment of the requirements for the degree of Doctor of Philosophy to the University of Minnesota in December 1959. Supported by the Electronics Components Laboratory of the Wright Air Development Center.

† Now at Rheem Semiconductor Corporation, Mountain View, California.

‡ Now at Institute for Crystal Physics, Melkweg 1, Groningen, the Netherlands.

[1] A. B. Laponsky and N. R. Whetten, Phys. Rev. Letters 3, 510 (1959).

[2] A. J. Dekker, Phys. Rev. Letters 4, 55 (1960).

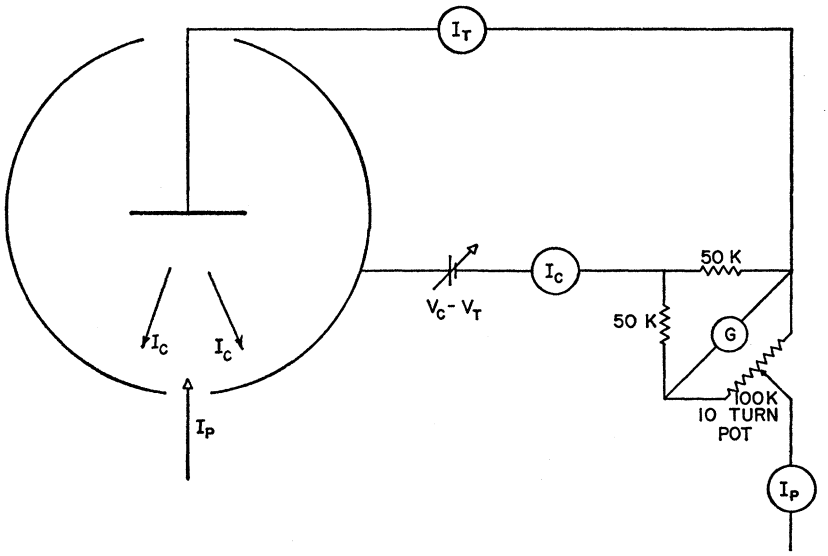

FIG. 1. Circuit for measuring δ.

The vacuum tube which was used in these measurements is sketched in Fig. 2. The envelope of the tube is made of Pyrex and is sealed to a Pyrex-enclosed titanium sputter pump, similar to Varian's Vac-Ion Pump. The principal parts of the tube are the electron gun, the collector, and the trolley. The electron gun is mounted on the bottom press and consists of 3 beam-forming electrodes and a tungsten filament. The collector sphere is supported by the bottom press through insulating rods, and is electrically connected to a press near the top of the tube. This allows the gun and collector to be accurately aligned and yet operate at large differences of potential without introducing electrical leakage. The collector has a small hole in the bottom for the electron beam, two holes in the sides for the trolley and crystal, and a hole in the top, covered with wire mesh, for observation. The observation hole is used to align the crystals with the beam and, in conjunction with a fluorescent target, to examine the focusing characteristics of the gun.

The trolley is made of stiff tungsten rods; it can be translated so that each crystal can be placed over the beam, and rotated through 360°. The center portion of the trolley is offset so that the front faces of the crystals lie in the axis of rotation. Also welded to the trolley are a nickel rotating lever and a mirror. This mirror is part of the system for measuring the angle of incidence of the primary beam. A fine line parallel to the trolley is inscribed on the face, and the plane of the mirror is parallel to the faces of the crystals. A cylindrical scale of 12-inch diameter is placed around the sidearm of the tube containing the mirror and is centered on the trolley. A point source of light is fastened to the cylinder directly above the mirror and illuminates the mirror. Thus, when the system is adjusted, an image of the scribed line falls on the cylindrical scale, which is

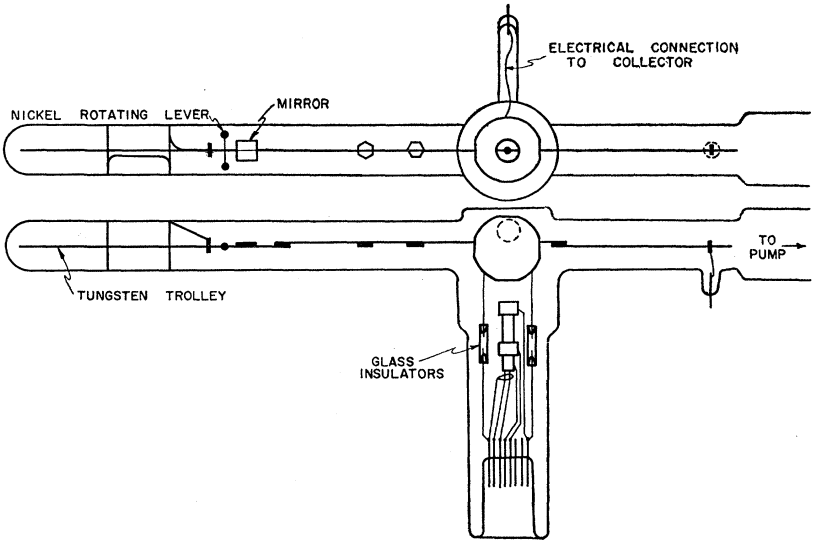

FIG. 2. The vacuum tube.

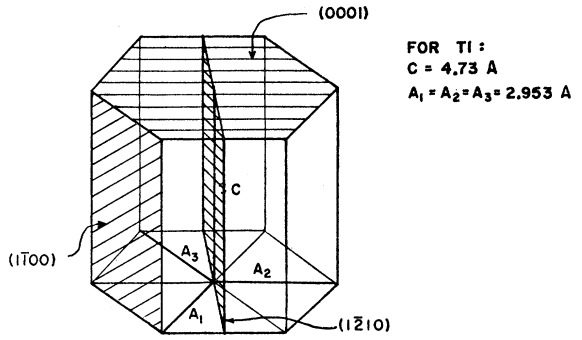

FIG. 3. The hexagonal close-packed structure of titanium.

marked off in degrees corresponding to the angle between the vertical and the normal to the mirror. The angle of incidence can be measured between $+60°$ and $-60°$.

The titanium crystals were purchased from the Chicago Development Corporation (Riverdale, Maryland). They were grown electrolytically and are said to be spectroscopically pure. The two single crystals which were selected each had a large (about 1 cm^2) flat face. The principal hexagonal directions were evident from the growth pattern of the crystals, and the flat faces were perpendicular to the **c** axis. The crystals were cleaned ultrasonically in a detergent-water solution, rinsed in hot 50% H_2SO_4, and cleaned ultrasonically in methanol before being put into the vacuum tube.

The variation of δ with θ was examined on the first crystal using a primary energy of 1020 ev. The curve showed negligible fine structure, about 10% of what was later found. Then this crystal was heated by rf induction to 750°C, brightness temperature, for one hour. The curve of δ vs θ was remeasured at 1020 ev and was found to exhibit quite prominent fine structure. All of the data on crystal No. 1 which are presented here were taken after this heating. Later crystal No. 1 was given a second, identical heating and the curve of δ vs θ was measured again. The second heating had no effect on the curves. Crystal No. 2 was given an identical heating before the data presented here were gathered.

Titanium crystals have the hexagonal, nearly close-packed structure shown in Fig. 3. Both of the crystals are bombarded upon the (0001) plane (the flat faces of the crystals) and the beam is parallel to the **c** axis when $\theta=0°$. As the crystal is rotated, the primary beam lies always in the plane which is perpendicular to the axis of rotation. Crystal No. 1 was oriented so that this is the (1$\bar{1}$00) plane shown in Fig. 3. In the case of crystal No. 2 the beam lies always in the (1$\bar{2}$10) plane shown in Fig. 3. The arrangement of the atoms in each of these planes is shown in Figs. 4 and 5 corresponding to crystals 1 and 2, respectively. Some of the principal zone axes are drawn in these figures and the angles they make with the **c** axis are indicated. The atoms in the (1$\bar{1}$00) plane are arranged symmetrically about the **c** axis. However, the atoms are not all symmetrically arrayed about the **c** axis in the (1$\bar{2}$10) plane.

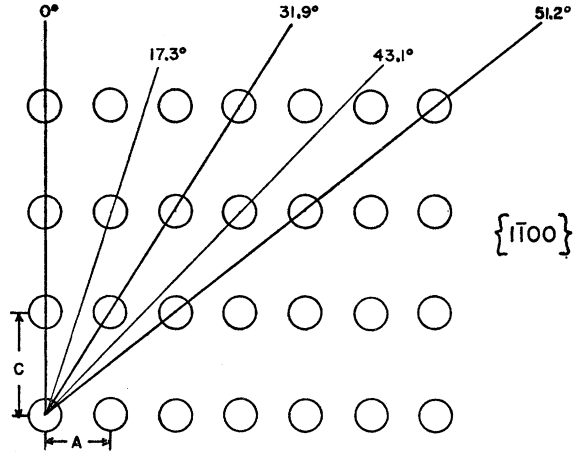

FIG. 4. The (1$\bar{1}$00) plane of the hcp Ti-crystal.

II. RESULTS

A. Crystal No. 1

The curves of the angular variation of δ are shown in Fig. 6 for primary energies of 120, 220, 520, and 1020 ev. The data points are shown for 120 ev because there is significant scatter in the data at this low primary energy. The data points are omitted from the other curves in

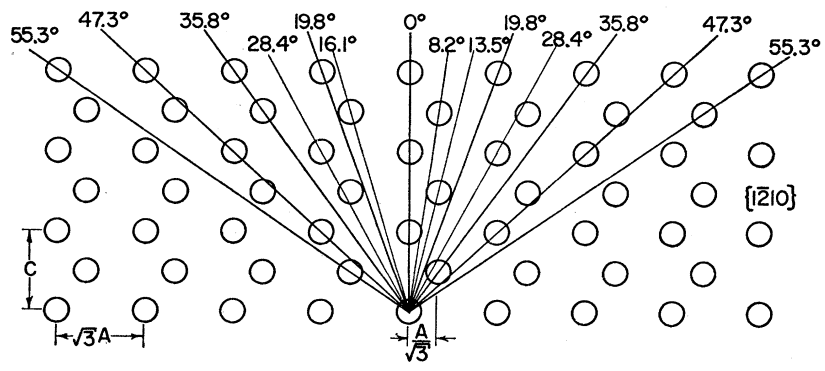

FIG. 5. The (1$\bar{2}$10) plane of the hcp Ti-crystal.

order to simplify them; in every case the curve is drawn through each datum point. For 220 and 520 ev the points were taken every 2° over straight portions and every 1° over curved portions. For curves at energies of 1020 ev and higher the measurements were made approximately every 0.5°. The curves for crystal No. 1 are symmetrical about the 0° line within the limits of the errors in the measurements.

It is apparent from a comparison of Figs. 4 and 6 that only the 0° peak is present when E_0, the primary energy, is 120 or 220 ev, but that the 31.9° and 51.2° peaks also appear at higher values of E_0. These fine-structure peaks will be designated by the angles which their corresponding zone axes make with the **c** axis even though the peaks are not always centered exactly on that angle. A striking feature of these curves is that the 0° peak has its largest value at a primary energy of 220 ev in spite of the fact that the other peaks have not yet developed. Note also that the width of the peaks is generally decreasing with increasing primary energy.

Measurements of δ vs θ were made for many values of E_0 in the range from 1120 ev to 12 kev. These curves are shown in Figs. 7, 8, and 9. It appears that the 17.3° peak (see Fig. 4) may also be present in these curves. As E_0 increases beyond 4 kev all the fine-structure peaks become narrower and smaller, and finally when E_0 is 12 kev the 0° and 51.2° peaks have vanished.

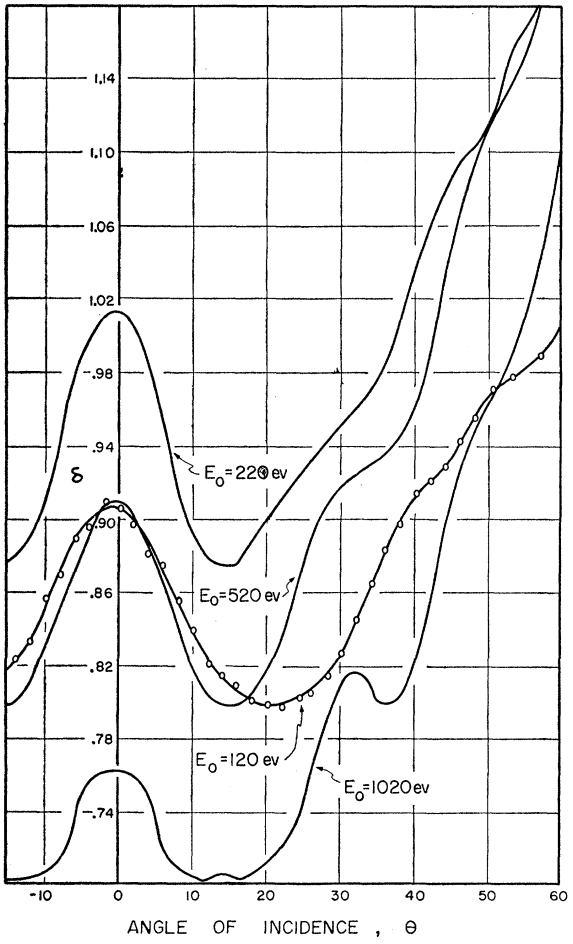

FIG. 6. δ as a function of the angle of incidence for $E_0=120$, 220, 520, and 1020 ev.

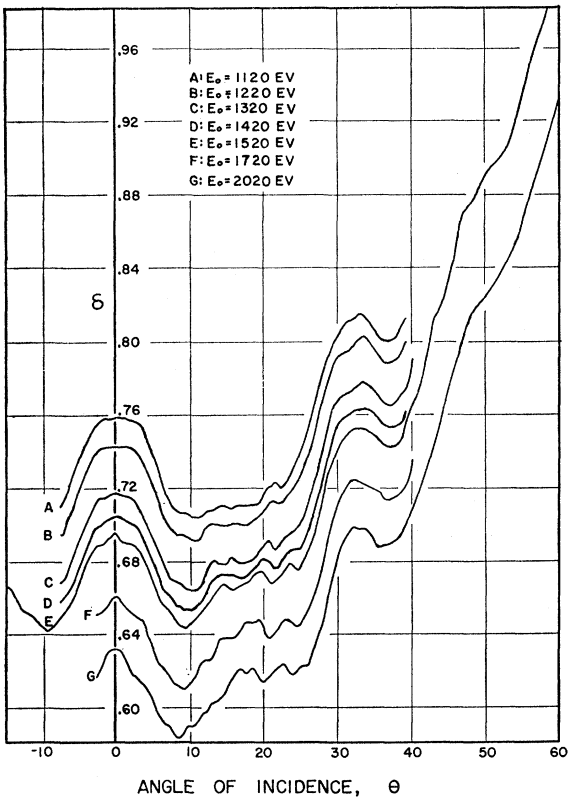

FIG. 7. Variation of δ with angle of incidence for values of E_0 between 1120 ev and 2020 ev.

In addition to the "normal," fine-structure peaks, the curves in Figs. 7, 8, and 9 also show a large number of small, very narrow peaks whose angular position varies with E_0. For convenience, these latter peaks will be called ultrafine structure (ufs). It appears that the ufs peaks even occur superimposed upon the normal peaks. (Note, for example, the shape of the 0° peak for $E_0=1520$ ev and the shape of the 31.9° peak for $E_0=4000$ ev.)

The data were taken at such energy intervals that the variation with energy of the magnitude and position of specific ufs peaks could be followed easily. The following examples illustrate the way in which the development of the ufs peaks may be traced:

(1) A ufs peak exists near 2.5° for $E_0=1120$ ev and shifts to about 3° for $E_0=1520$ ev (Fig. 7).

(2) A ufs peak begins at about 23.5° for $E_0=1520$ ev, shifts to 21.5° at 2500 ev and to 21° at 3500 ev, and then disappears (Figs. 7 and 8).

(3) A ufs peak begins at 24° for $E_0=3000$ ev, reaches maximum height at 23.5° and 3750 ev, and is diminishing at 23° and 5000 ev (Figs. 8 and 9).

(4) A ufs peak is present near 11.5° when E_0 is 3250, 3500, 3700, 3750, and 4000 ev (Fig. 8).

(5) The structure in the neighborhood of 8° for high E_0 might be considered to consist of 3 peaks, the first around 6.5° when E_0 is 3000, 3250, 3500, and 3750 ev, the second around 8° when E_0 is 3750, 4500, and 5000 ev, and the third around 9° when E_0 is 4500, 5000, 6000, and 7000 ev (Figs. 8 and 9).

A study was also made of the energy distribution of the secondary electrons which comprise the fine-structure peaks. This distribution was the same as that of the normal secondaries, except for the presence of a relatively large number of nearly elastically backscattered primaries. For the 0° peak when $E_0=520$ ev, for example, about 3% of all primary electrons are reflected; this comprises about 36% of the magnitude of this peak.

The variation with primary energy of the magnitude of the 0° peak is shown in Fig. 10. The data are presented in the form of a ratio of the magnitude of the peak to that of the corresponding gross effect. This gross effect is determined by estimating a smooth base curve; the magnitude of the fine-structure peak is measured from this base curve. Although this method is somewhat ambiguous, it is certainly adequate to illustrate the trends. The prominent features of this curve is the large, narrow maximum near 200 ev and the gradual decrease at high values of E_0.

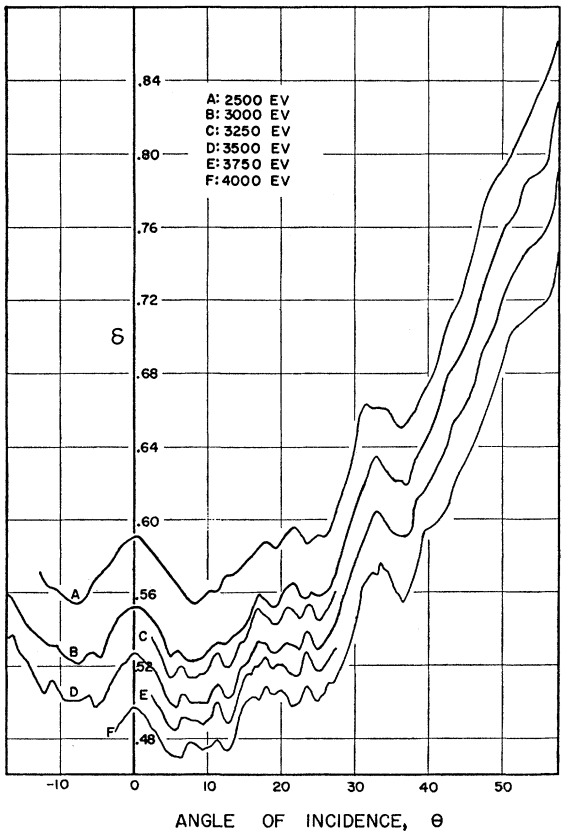

FIG. 8. Variation of δ with angle of incidence for values of E_0 between 2500 ev and 4000 ev.

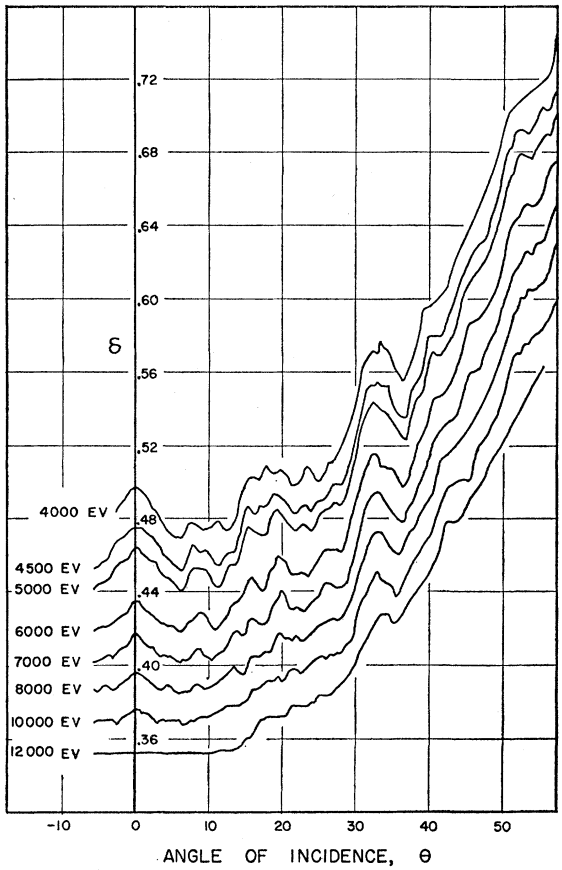

FIG. 9. Variation of δ with angle of incidence for values of E_0 between 4000 and 12 000 ev.

B. Crystal No. 2

Crystal No. 2 was oriented on the trolley so that the primary beam would always lie in the $(1\bar{2}10)$ plane (see Fig. 3). The possible alignments of the beam with prominent zone axes are shown in Fig. 5. These zone axes are not symmetrical about the **c** axis and this basic asymmetry appears to be the source of asymmetry in the data. The curves of δ vs θ for crystal No. 2 are shown in Fig. 11 when E_0 is 520, 1000, and 2000 ev. Note that the asymmetry occurs only at the higher energies; the curve for $E_0=520$ ev is quite symmetrical. It is probably best to emphasize here that measurements were made on crystal No. 1 at both high and low energies for θ between $+60°$ and $-60°$ and that the curves are symmetrical.

Although this asymmetry is not fully understood, it is felt that it is a consequence of the asymmetrical arrangement of the atoms about the **c** axis. Such an explanation requires a rather unusual assumption, however, because the asymmetry shown in Fig. 5 would

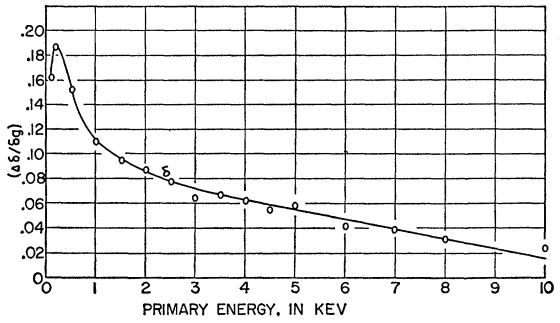

FIG. 10. Dependence of the magnitude of the fine structure on primary energy.

appear in the reverse fashion if the top atom layer of the hcp structure were removed. Thus in order for the asymmetrical arrangement of the atoms to cause the asymmetrical data it would be necessary for one of the two types of layers to predominate on the surface of the crystal. Since the atom layers in the titanium structure are perfectly equivalent, this seems like a rather unlikely situation. It is possible, of course, that there is something in the mechanism of growth of these crystals (or in their vacuum annealing) which promotes this situation. (This unusual assumption continues to be necessary even if the crystal is considered to be misaligned on the trolley, because any asymmetry resulting from misalignment would appear in the reverse fashion upon removal of one atom layer.) This aspect of the experiment should be explored further.

III. INTERPRETATION

A. The "Normal" Fine Structure

Both the "normal" fine structure and the ultrafine structure are thought to be caused by coherent elastic scattering, i.e., electron diffraction, of the primary electrons. This model has been described previously[2] in some detail by one of the authors, and consists essentially of the following: The primary electrons will move into the crystal a distance which is of the order of the mean free path for inelastic scattering before their wavelengths have been changed sufficiently to make them unable to cooperate in coherent elastic scattering. This distance will be very much less than the total penetration depth. Thus, in this model the primary beam is first diffracted by a crystal which is only a few atoms thick, and then the diffracted beams and the remainder of the undeflected beam enter the macroscopic crystal and produce secondary electrons. Transmission electron diffraction patterns of extremely thin crystals were first observed by Kikuchi,[3] and consist of an array of small spots clustered about the central spot which is formed by the undiffracted beam. A pattern of this type appeared whenever the primary beam was incident along one of the principal zone axes of the thin crystal. So in the present case, whenever the primary beam is incident along one of the principal zone axes a large number of diffracted beams will be formed which will make larger angles with the normal to the surface, and will therefore increase the δ.

In the previous paper,[2] an expression was derived for the fraction of the primary beam which is diffracted into a given direction. This was done by means of the first-order kinematic theory in which it is assumed that the decrease in intensity of the incident beam due to diffraction is negligible, and that any further scattering of a diffracted beam is also negligible. These assumptions would be justified if elastic scattering of electrons by atoms were a slight effect, but this is not the case. In fact, using reasonable numerical values in this expression, one finds that a large fraction of the incident electrons are diffracted. The dynamical theory of electron diffraction[4] might be fruitfully applied to this problem, since it does take into account the effects of multiple scattering.

Although the simple kinematic theory is inadequate for a detailed comparison of the results with the data, it does show that the diffraction effect is very significant, and it explains qualitatively many characteristics of the fine structure. It predicts the existence of fine-structure peaks whose positions correspond to the zone axes and are independent of E_0. The magnitude of the calculated peaks are of the same order as those observed, and vary in the same way with E_0.

The simple theory also predicts the presence of a

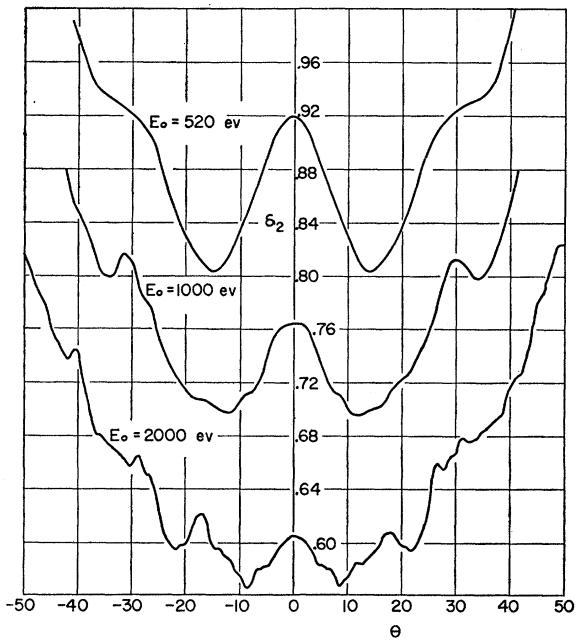

FIG. 11. Secondary yield of crystal No. 2 versus angle of incidence.

[3] S. Kikuchi, Physik. Z. **31**, 777 (1930), Plate No. 24.

[4] J. J. Thomson, Phil. Mag. **8**, 1073 (1929); P. M. Morse, Phys. Rev. **35**, 1310 (1930); S. Kikuchi, Sci. Papers Inst. Phys. Chem. Research (Tokyo) **26**, 225 (1935); H. A. Bethe, Ann. Physik **87**, 55 (1928).

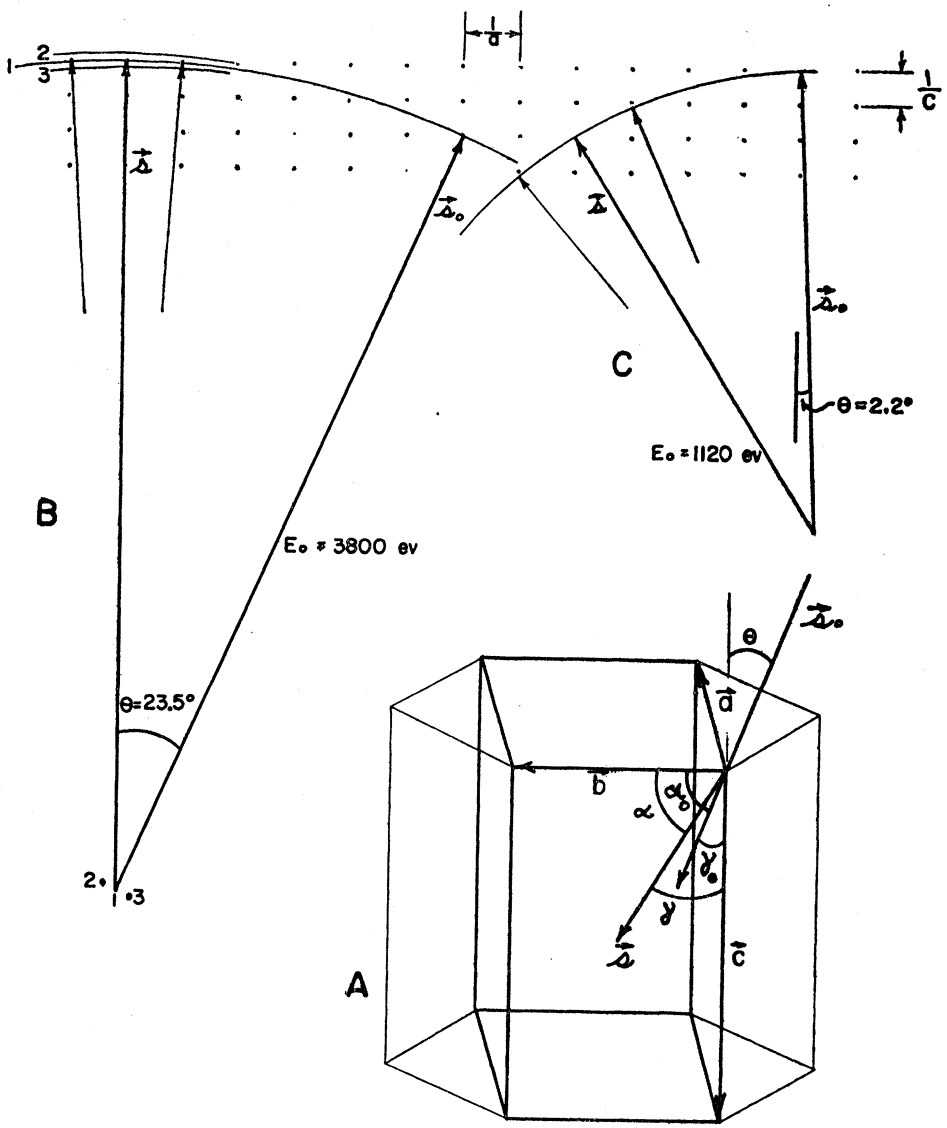

FIG. 12. (a) The orthohexagonal unit cell; (b) and (c) Ewald's construction for the ultrafine structure.

measurable number of primaries scattered out of the crystal with essentially no energy loss. A lattice of scattering points would scatter in an identical manner in both the forward and backward directions; however, a real crystal scatters more weakly in the backward direction because the atomic scattering factor decreases with increasing values of the scattering angle. The sum of all back-diffracted electrons has been computed for $E=500$ ev and is about 1%, in approximate agreement with the measured value.

The fact that the 0° fine-structure band is larger than the others can also be understood on the basis of the simple theory. When the primary beam is normally incident on the crystal, every diffracted beam necessarily increases δ; whereas for fine-structure peaks at larger angles of incidence a few of the diffracted beams will lower δ and decrease the magnitude of the peak. The decreasing width of the fine-structure peaks with increasing E_0 is also in agreement with the theory, because as E_0 increases, the extensions of the reciprocal lattice points decrease, and the range of primary angles for which the reflection sphere cuts the extended points in a given plane decreases.

B. The Ultrafine Structure

It appears that the ufs peaks are also caused by diffraction of the primary electrons, although in this case multiple diffraction is involved. Applying the Laue equations to the titanium lattice we can calculate the location, in energy and angle, of some of the ufs peaks, but not their magnitude.

In this work only the ufs of crystal No. 1 will be considered. The orthohexagonal unit cell, shown in Fig. 12(A), will be employed. For crystal No. 1 the incident beam, $\mathbf{s}_0$, always lies in the plane of **a** and **c**,

TABLE I. Some ultrafine-structure peaks.

γ	h, l	θ_{max}	$E_{0\,max}$ (ev)	Shift of θ as E_0 increases
0°	6, −2	23.5°	3800	θ decreases
31.9°	4, 2	2.2°	1120	θ increases
31.9°	−12, 4	9.0°	5320	θ decreases
51.2°	14, 8	12.0°	3470	θ decreases
51.2°	14, 6	21.3°	2580	θ decreases

and only diffracted beams, **s**, which also lie in this plane will be considered. (This restriction automatically limits this consideration to a small fraction of the possible ufs peaks.) Thus the Laue equation which describes phase relations along the **b** direction is always satisfied. Since $\theta=\gamma_0$ and α and γ are related (either $\alpha+\gamma=90°$ or $\alpha-\gamma=90°$), the remaining two Laue equations are

$$\begin{aligned} a(\pm\sin\gamma-\sin\theta)&=h\lambda,\\ b(\cos\gamma-\cos\theta)&=l\lambda, \end{aligned} \tag{1}$$

where the (+) holds if α is less than 90° and the (−) if α is greater than 90°. These equations specify the relations between γ, θ, and λ when all the atoms in the crystal scatter exactly in phase. The presence of atoms within the unit cell imposes the condition that h and l be even.

In this model some of the ufs peaks are thought to develop when Eqs. (1) are satisfied for diffraction into one of the "normal" fine-structure directions, i.e., when γ is 0°, 31.9° or 51.2°. Table I shows some of the sets of values of γ, h and l, θ, and E_0 which satisfy Eqs. (1). Note that these sets of values of θ_{max} and $E_{0\,max}$ are almost identical to those of some of the principal ufs peaks described above. From the Bragg condition for diffraction

$$2d_{hkl}\sin\theta_B=\gamma$$

we see that as E_0 increases, the Bragg angle always decreases. If **s** and $\mathbf{s}_0$ are on the same side of the **c** axis, then the measured θ decreases as θ_B decreases, but if **s** and $\mathbf{s}_0$ are on opposite sides then θ increases as θ_B decreases. The predictions of this argument for the direction of shift of θ with increasing E_0 are also given in Table I. These directions agree with the data in every case, except for the fourth entry where the direction of shift is not evident from the data.

The reason why diffraction into the directions corresponding to the normal fine-structure peaks results in especially prominent ufs peaks can be seen most clearly by employing Ewald's construction[5] in the reciprocal lattice. This construction is shown in Fig. 12, *B* and *C*, for the first two ufs peaks listed in Table I. Figure 12 shows that, when the conditions are satisfied for diffraction into the direction of a zone axis, they will be nearly satisfied for diffraction into the directions which make small angles with that zone axis. Thus the ufs peaks might be thought of as being the superposition of four or more smaller peaks upon the larger peak which exactly satisfies the Laue equations.

It is possible to show by means of Ewald's construction that this model does produce extremely narrow bands. Figure 12(B) shows the complete construction, labeled "2" and "3", for the same E_0 but for θ values of 24.5° and 22.5°, respectively. Since at this energy the reciprocal lattice points are extended only 1/19 of the way to the next point (assuming $N_3=E_0/200$), the spheres 2 and 3 will not cut any of the extensions near the zone axis. So this ufs peak should be significantly narrower than 2°, and any ufs peaks occurring at a higher energy should be narrower still. However, the data do not show any ufs peaks of width less than about 2°. This minimum width exhibited by the data is probably a consequence of the divergence of the primary beam. The ufs peaks do appear to be much wider at low primary energies, as is required by this model.

There are a great many small peaks and dips in the curves which have not been associated here with specific reflecting planes and diffracted directions. However, considering the large number of possible intersections of the reflection sphere with the extended lattice points, it seems possible that all of the ufs in the data might be caused by this effect.

Fine-structure and ufs peaks would never appear in data taken on a material consisting of randomly oriented crystallites. However, the diffraction phenomena would still occur, and would contribute significantly to the spreading out of the primary beam in the initial part of its path. It may well be necessary to take into account this additional spreading due to diffraction in future theories of secondary emission from polycrystalline solids.

[5] P. P. Ewald, Z. Krist. **56**, 129 (1921); Physik. Z. **14**, 465, 1038 (1913). M. von Laue, Jahrb. Radioakt. u. Elektronik **11**, 308 (1917).